

PS Controls of Structural Inheritance in Normal Fault Propagation and Extensional Basin Segmentation: The Crati Basin, Northern Calabria, Italy*

Vincenzo Spina¹, Emanuele Tondi², and Stefano Mazzoli³

Search and Discovery Article #40884 (2012)

Posted February 27, 2012

*Adapted from poster presentation at AAPG International Convention and Exhibition, Milan, Italy, October 23-26, 2011

¹Geosciences Division, TOTAL E&P Italia, Rome, Italy (spinavincenzo@yahoo.it)

²Earth Sciences, University of Camerino, Camerino, Italy

³Earth Sciences, University of Naples "Federico II", Naples, Italy

Abstract

The western sector of the Calabrian Arc is considered a classic extensional domain that developed as a result of subduction rollback and related back-arc opening since Late Miocene times.

However, the development of the back-arc domain is controlled by major strike-slip faults related to the heterogeneous nature of the Adria lithosphere and accommodating the SE migration of the Calabrian Arc. Since Middle Miocene to Lower Pleistocene, en-échelon NW-SE oriented left-lateral strike-slip faults exerted a major control on the tectonic evolution of northern-central Calabria. A series of extensional basins also developed in the area since the Plio-Pleistocene, being linked with, and segmented by these strike-slip faults.

The Crati Basin developed in the northern portion of the Calabrian Arc, being filled by Tortonian to Lower-Middle Pleistocene marine to deltaic deposits. Strike-slip faults and associated shortening at contractional jogs affected the basin fill during the early stages of its evolution. Since the Middle Pleistocene, N-S striking normal faults began to form, controlling the basin architecture.

The tectonic evolution of the Crati Basin has been investigated by the integration of field mapping, the construction of geological cross sections and bio-stratigraphic analyses with the interpretation of 2D seismic data. Seismic interpretation, used to constrain the structure of the basin at depth, confirmed that the master fault of the extensional fault system controlling the Crati Basin is represented by a blind fault dipping towards the west. This indicates that the Crati Basin may be interpreted as a half-graben that formed since

Middle Pleistocene time. A minimum value of cumulative vertical displacement of ca. 600 m has been unraveled for the central sector of the Crati Basin since Middle Pleistocene times. This yields a vertical strain rate of ca. 0.9 mm/y during the last 700 ka.

Normal faults started to develop in the southernmost sector of the basin, where they abut against pre-existing strike-slip faults. It is envisaged that strike-slip faults, becoming progressively inactive and working as persistent barriers, inhibited the propagation towards the south of the newly formed normal faults, which therefore propagated towards the north, where such barriers were absent.

Controls of structural inheritance in normal fault propagation and extensional basin segmentation: the Crati Basin, northern Calabria, Italy.

Spina, V. (1); Tondi, E. (1); Mazzoli, S. (2);

(1) Dipartimento di Scienze della Terra, Università di Camerino, Italy. (2) Dipartimento di Scienze della Terra, Università di Napoli "Federico II"

Introduction

The Western sector of the northern Calabria is considered a classic extensional domain that developed as a result of subsiding rollover and related back-arc opening since Late Miocene times (e.g. Malinverno and Ryan, 1986). Although various Authors highlighted the importance of extensional tectonics in northern Calabria, no agreement exists on its timing. The peculiar modes of development of the Tyrrhenian Sea, controlled by major strike-slip faults accommodating the SE migration of the Calabrian Arc, produced a rather complex tectonic setting (Knoet and Turco, 1991). This is characterized by large lateral displacements along NW-SE striking wrench faults (Van Dijk et al., 2000), that are well beyond those typically associated with transfer faults in classic extensional settings. In northern Calabria, in particular, large left-lateral motions along NW-SE lineaments may be associated with geodynamic processes involving the whole subducting slab, with a lithospheric tear starting to develop at ca. 2.5 Ma in this area (Chiarabba et al., 2008). The Crati Basin (CB), located in the western side of northern Calabria, is traditionally included in the back-arc domain of the Ionian subduction system. The tectonic evolution of the CB and its relationships with the opening of the Tyrrhenian Sea and development of the southern Apennines and the Calabrian Arc are still a matter of debate (Tortorici et al., 1995; Mattei et al., 2002, 2007; Cifelli et al., 2006; Tansi et al., 2007; Pepe et al., 2010). The CB is bounded to the south and to the north by long-lived NW-SE trending left-lateral strike-slip faults (Fig. 1). Strike-slip tectonics affected the central-southern Apennines and the Calabrian Arc at different times (Cello and Mazzoli, 1999; Tondi, 2000; Van Dijk et al., 2000; Cello and Cello, 2003 and references therein). In the Calabrian Arc NW-SE oriented left-lateral strike-slip faults and associated jog-related features (i.e. folds, reversed normal faults) controlled the evolution of the belt since Late Miocene times (Knoet and Turco, 1991; Van Dijk et al., 2000, and references therein). Recently, Tansi et al., 2007 described transpressive structures formed at compressive jogs related to NW-SE left-lateral strike-slip faults dated as probably Early Pliocene in the southernmost sector of the CB. Further evidence of Neogene shortening in the Tyrrhenian sector of the Calabrian Arc have been recently shown by Pepe et al. (2010). We investigate the Miocene to Present space-time evolution of the tectonic structures affecting the Crati basin. This is carried out by integrating geological field data with seismic reflection profiles of various resolutions, calibrated by deep wells. The proposed model contextualizes the evolution of the CB in the regional framework of the western margin of northern Calabria where a series of basins, segmented by the previously mentioned strike-slip structures, occur both offshore (i.e. the Gioia Basin; Sartori, 1989, 1990) and onshore (i.e. the Messina Graben; Lanzafame and Tortorici, 1981; Tortorici, 1981; Tansi et al., 2005).

Regional geological setting

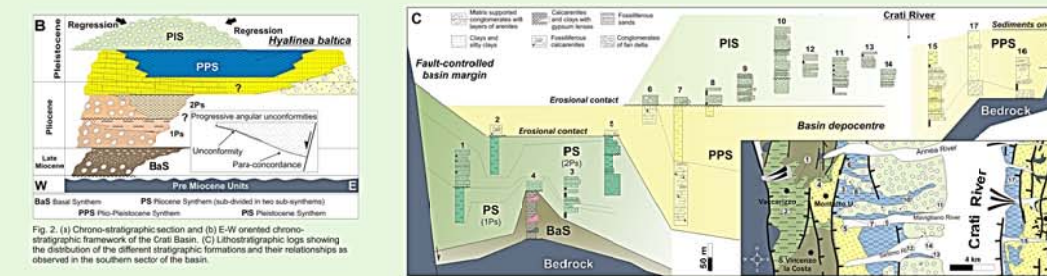
The CB is a tectonic depression located in the western sector of northern Calabria, geologically representing part of the Calabrian Arc (Fig. 1). The Calabrian Arc consists of a series of thrust nappes composed of tectonic units deriving from the deformation of different palaeogeographic domains since the Oligocene times (Dewey et al., 1989; Bonardi et al., 2001; Rossetti et al., 2001; Mattei et al., 2002; Bonardi et al., 2005; Iannace et al., 2005). The evolution of the Calabrian Arc is characterized by a progressive southeastward migration since Miocene times, associated with Africa-Europe major plate convergence (e.g. Mazzoli and Helman, 1994) and occurring along a NW-SE to NNW-ESE-trending regional strike-slip faults (Fig. 1; Ghisetti and Vezzani, 1982; Turco et al., 1990; Knoet and Turco, 1991; Catalano et al., 1993). Since the Middle Pleistocene, a strong and still active regional uplift started to affect the northern Calabrian Arc. This has been interpreted as the isostatic response to the removal of the high-density mantle lithosphere root, due to detachment of the Ionian subducted slab (e.g. Wortel and Spackman, 1993; Tortorici et al., 1995). According to these Authors, the regional uplift was coupled with the formation of a series of grabens along the entire western sector of the Calabrian Arc. The CB, forming part of this zone, is bounded by the Coastal Range to the west, by the Sila Massif to the east, and by the Pollino Ridge to the north (Fig. 1). The basin is morphologically asymmetric with a steeper and shorter fluvial drainage along its eastern border, and the Crati River flowing along the easternmost side of the valley.

Basin stratigraphy

The CB is filled by Upper Miocene to Holocene clastic marine and fluvial deposits (Fig. 2, see also Vezzani, 1968; Coella et al., 1987) covering the Palaeozoic crystalline bedrock, in the southern part of the basin, and Meso-Cenozoic carbonates in its northern sector (i.e. in the Pollino area). Although the main depocentre is located in the northernmost sector of the basin (Sibari Plain, Fig. 1), the thickness of the deposits increases from the Coastal Range towards the Sila foothills (Fig. 2).

Basal Synthem (BaS). The BaS consists of conglomerates gradually evolving upwards to sands and arenites. The latter sediments, in turn, give way upwards to clays and silty clays, and then to Messinian evaporites (Lanzafame and Tortorici, 1981). The thickness of the BaS is variable; Lanzafame and Tortorici (1981) suggested 250 m; however, the whole thickness increases to the north as confirmed by subsurface data.

Pliocene Synthem (PS). The PS consists of two thinning-upward sub-syntheses bounded by discontinuities and depositional hiatuses (Fig. 2), cropping out mainly along the western border and the northernmost part of the CB (Fig. 3). Sediments of the first interval (1PS) consist of cross-bedded continental conglomerates, progressively evolving upwards to sands with planar bedding. Marine clays characterize the top of the interval. Biostratigraphic analyses suggest a Zanclean age for these sediments. Sediments of the second sub-synthem (2PS) overlie both the Miocene and the Lower Pliocene deposits (Fig. 3). To the south, 2PS are characterized by fluvial and fan-delta conglomerates evolving, towards the axial part of the basin, to marine silty clays. Biostratigraphic analyses point out a Piacenzian age. In the northernmost part of the basin (Fig. 3 a), marine silty clays overly Messinian deposits or Mesozoic carbonates. Based on surface data, the 2PS can be estimated as ca. 400 m thick (see also Russo and Schiattarella, 1992).



Plio-Pleistocene Synthem (PPS). In the southernmost sector of the CB, the bottom of PPS is mainly characterized by fossiliferous calcarenites with planar cross bedding; however, along the Sila foothills, this succession starts with conglomerates evolving upwards to thin sands (Fig. 2). All such deposits grade into marine silty clays, cropping out in the axial and main depocentral sector of the basin (Fig. 2). Geological considerations and the occurrence of Hylinea balica unraveled by new analyses allow assigning an Emilian age (biozone Globigerinoides quadrilobatus) to these clays. In the northernmost part of the CB, coarse-grained sediments overlying the Pliocene clays crop out in the peripheral areas of the basin (Fig. 3 a) and along the Ionian coast of Calabria (Vezzani, 1968). The thickness of the PPS increases towards the Sibari Plain, as shown also by deep wells for hydrocarbons exploration.

Pleistocene Synthem (PIS). These deposits crop out along the axial part of the basin and, more extensively, in the Sibari Plain. This synthem consists of Gilbert-type marine fan delta deposits (Coella, 1988), which prograded into small fault-controlled sub-basins within restricted gulfs and narrow embayments of the CB. PIS deposits show an erosional contact with older deposits in the peripheral sectors of the southern part of the CB (Fig. 2), but they rest conformably onto the Lower Pleistocene clays in the axial part of the basin. Based on the stratigraphic relationships with underlying deposits, we suggest an Early-Middle Pleistocene age for the fan delta conglomerates. The observed thickness for this interval, is about 150 m and increases towards the north.

Middle Pleistocene cryoclastic breccias (Fig. 3) also occur along the foothills of the Pollino Range. In the Sibari Plain (Fig. 3a) the fan delta conglomerates pass upwards to Upper Pleistocene lacustrine/palustrine sediments, clearly pointing out the regressive trend of this interval. Lacustrine sediments attain a maximum thickness of about 100 m.

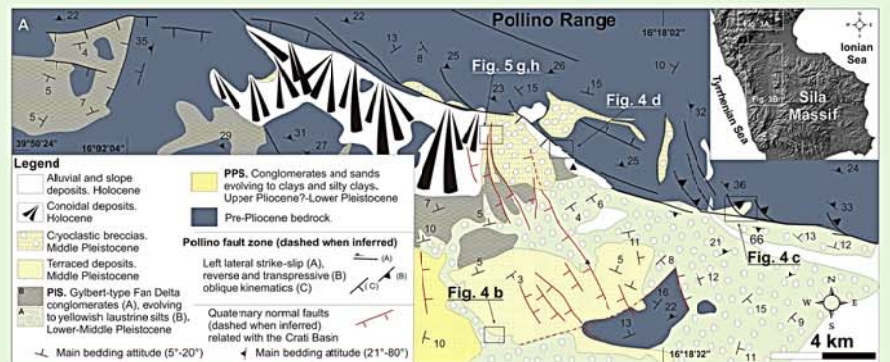
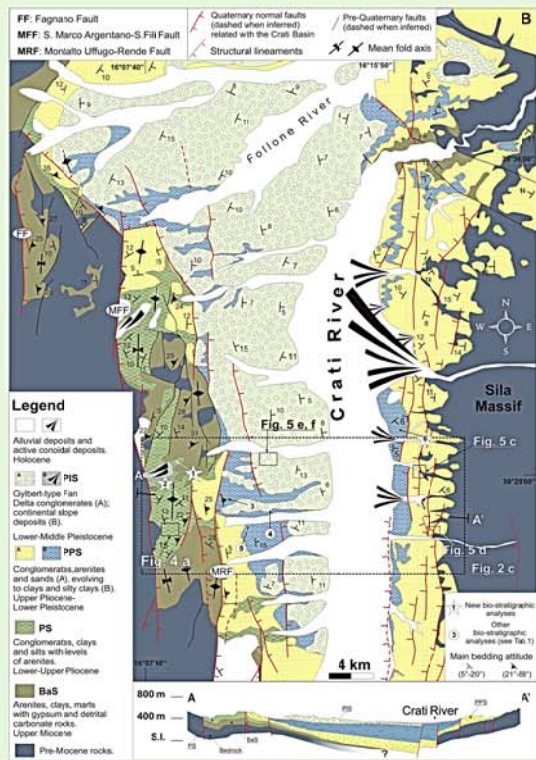


Fig. 3. Geological maps of the Crati Basin. (a) Northern sector of the basin (Pollino area). (b) Southern and central sectors of the basin.

Structures

Compressional and extensional structures deform sediments of different age within different sectors of the CB. In the southern and central part of the basin, roughly N-S trending folds (Fig. 4a) involve sediments of Miocene and Lower Pliocene age (up to the 1PS). In the northern sector of the basin, minor high-angle reverse faults affect Lower Pleistocene fan delta conglomerates (Fig. 4b). Along the Pollino Fault Zone, Mesozoic carbonates are locally brought into contact with Lower-Middle Pleistocene conglomerates by means of high-angle reverse faults (Fig. 4c). Minor NW-striking, left-lateral strike-slip faults have been observed within the Early Pleistocene breccias (Fig. 4d). Notwithstanding the occurrence of such minor structures the morphology of the CB is clearly controlled by a N-S trending structural grain along both sides of the basin abutting against long-lived strike-slip fault zones (Fig. 5a, b). The western border of the basin is characterized by three main N-S striking, E-dipping normal faults (Fig. 5) arranged in an en-echelon geometry, in the central and southern sectors, also the eastern border of the basin is characterized by a series of N-S oriented faults (Figs. 5c, d). Instrumental seismicity and medium-intensity historical earthquakes cluster along these structures, which have been interpreted as active faults (Tansi et al., 2005; Spina et al., 2009). The morphological offset of the faults bordering the western side of the basin (i.e. the height of the steepest part of faceted spurs, see Fig. 5a) ranges between 60 m and 230 m (see also Tortorici et al., 1995; Spina et al., 2009), with the highest values clustering in the central part of the array and the minimum values occurring at relay ramps. Along the eastern border of the basin the morphological offsets observed along faults range between 50 m and 170 m, decreasing rapidly to 0 towards the Pollino Range (Fig. 5g). Extensional structures, also oriented mainly N-S, also affect the interior part of the basin and cross-cut, at the meso-scale, compressional structures deforming the basin infill. In the southern sector of the CB, normal faults show evidence for syn-sedimentary activity (Fig. 5e, f), in the axial zone of the basin.

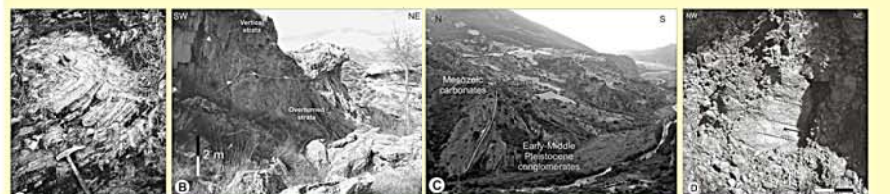


Fig. 4. Field examples of contractional and strike-slip structures affecting the basin infill (see Fig. 3 for location).

A structural survey has been carried out in order to investigate in detail the kinematics of the extensional faults. In the southern and central sectors, the faults detected structures include faults showing dip angles in the range of 50°–70° (Figs. 5, 6) mainly striking NNW–SSE and NNE–SSW. All together, the collected faults show oblique-slip to pure dip-slip kinematics, with pitch values ranging between 55° and 90° (Fig. 6). No consistent superimposition of strike/shear fibres has been observed on fault planes, thus suggesting that no major switch of the regional stress field occurred in this area after the formation of these structures. The direction of extension in this part of the CB, as shown by fault slip inversion for paleostress analysis (Reches, 1987), is sub-horizontal and oriented E–W (Fig. 6). The low value of the axial ratio ($R=0.22$), suggests a geometry of the stress field characterized by similar values of σ_2 and σ_3 .

In the northern part of the CB normal faults cross-cut compressional structures and affect sediments of Middle-Late Pleistocene age. Rose diagram shows a mean peak strike value of N348°E (Fig. 6). These normal faults are characterized by oblique-slip kinematics showing a left-lateral component of motion (see Figs. 5h, 6). Inversion of fault slip data point out a sub-horizontal, NNE–SSW oriented maximum extension direction in the northernmost part of the CB (Fig. 6). The low value of the axial ratio ($R=0.12$) indicates a geometry of the stress ellipsoid similar to that characterizing the southern part of the basin.

In the same area, these faults exhibit an elliptical profile of displacement (Fig. 5g) as they lose their morphological evidence approaching the Pollino Fault Zone (Fig. 5). Pitch and asymmetric profile of displacement are characteristic of the tip zones of basin-bounding normal faults.

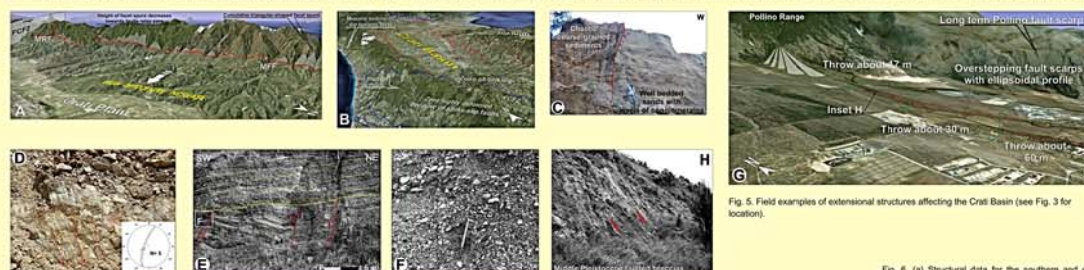


Fig. 5. Field examples of extensional structures affecting the Crati Basin (see Fig. 3 for location).

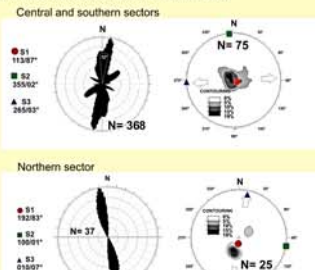


Fig. 6. (a) Structural data for the southern and central sectors and (b) for the northernmost part of the Crati Basin.

Subsurface data

Sparse subsurface data are available for the CB. Well logs were used to assess the thickness of sedimentary formations in this sector. Four 2D seismic lines, that were shot about twenty years ago for HC exploration, are also available. Due to the relatively poor quality of the lines, their wide spacing and limited area coverage, this dataset does not allow fully constraining the structures in 3D (i.e. defining precisely fault strike and length) throughout the entire basin. Nevertheless, these data are useful to describe the overall subsurface geometry of the CB and the structures controlling the basin architecture. Three NE–SW oriented seismic reflection profiles are available across the Sibari Plain. They have been calibrated using the wells that were drilled in order to test Miocene structural traps and shallower Plio-Quaternary targets (Fig. 7). A further seismic line, roughly oriented E–W and almost orthogonal to the major structures bordering the CB, allowed us investigating also subsurface structure of the central portion of the basin (Fig. 7). However, while seismic lines could be tied to well logs in the northernmost part of the basin to constrain geological horizons, no exploration wells are present in the central sector of the basin and no offset exists between seismic lines in this area and to the north. Therefore, we used surface information (i.e. the geological map) and the characteristics of the seismic facies to differentiate between major stratigraphic units in the central basin area. Despite this approximation, basin architecture, type and overall kinematics of the structures deforming the basin fill could still be recognized with confidence.

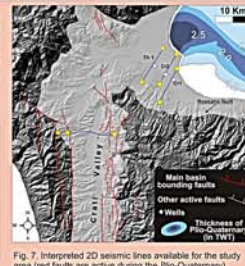
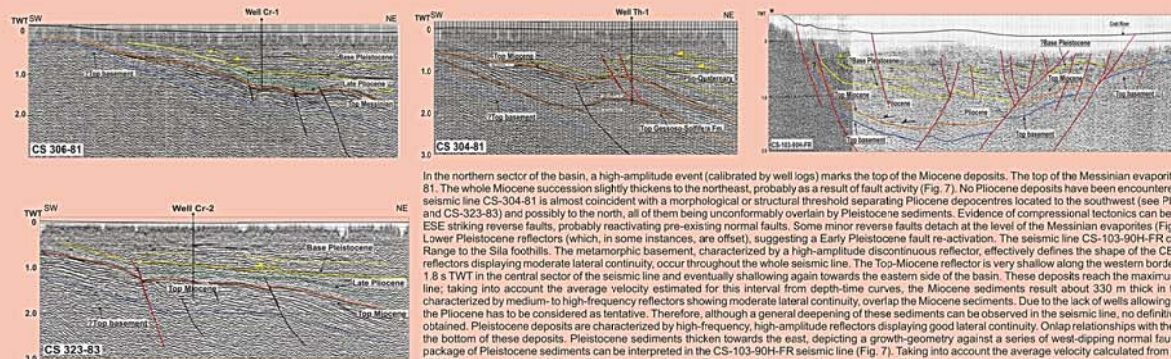


Fig. 7. Interpreted 2D seismic lines available for the study area (red faults are active during the Plio-Quaternary).

In the northern sector of the basin, a high-amplitude event (calibrated by well logs) marks the top of the Miocene deposits. The top of the Messinian evaporitic sediments can also be recognized in the line CS-304-81. The whole Miocene succession slightly thickens to the northeast, probably as a result of fault activity (Fig. 7). No Pliocene deposits have been encountered in the well Thuro-1 (see Fig. 7). This suggests that the seismic line CS-304-81 is almost coincident with a morphological or structural threshold separating Pliocene depocentres located to the southwest (see Pliocene horizons recognized in seismic lines CS-306-81 and CS-323-83) and possibly to the north, all of them being unconformably overlain by Pliocene sediments. Evidence of compressional tectonics can be recognized in the seismic lines showing roughly WNW–ESE striking reverse faults, probably reactivating pre-existing normal faults. Some minor reverse faults detach at the level of the Messinian evaporites (Fig. 7). Reverse faulting also produced deformation of the Lower Pleistocene reflectors (which, in some instances, are offset), suggesting a Early Pleistocene fault re-activation. The seismic line CS-103-90H-FR crosses the central sector of the basin, from the Coastal Range to the Sila foothills. The metamorphic basement, characterized by a high-amplitude discontinuous reflector, effectively defines the shape of the CB. Miocene sediments, characterized by high-amplitude reflectors displaying moderate lateral continuity, occur throughout the whole seismic line. The top-Miocene reflector is very shallow along the western border of the basin (i.e. Coastal Range foothills), deepening to 1.8 s TWT in the central sector of the seismic line and eventually shallowing again towards the eastern side of the basin. These deposits reach the maximum thickness (ca. 0.25 s TWT) in the central sector of the line; taking into account the average velocity estimated for this interval from depth-time curves, the Miocene sediments result about 330 m thick in the main basin depocentre area. Pliocene sediments, characterized by medium-to-high-frequency reflectors showing moderate lateral continuity, overlap the Miocene sediments. Due to the lack of wells allowing tying with the seismic line, the interpretation of the top of the Pliocene has to be considered as tentative. Therefore, although a general deepening of these sediments can be observed in the seismic line, no definitive information about the thickness of this interval can be obtained. Pliocene deposits are characterized by high-frequency, high-amplitude reflectors displaying good lateral continuity. Onlap relationships with the underlying strata have been tentatively used to identify the bottom of these deposits. Pliocene sediments thicken towards the east, depicting a growth-geometry during a series of well-dipping normal faults. Based on such assumptions, a ca. 1.3 s TWT thick package of Pliocene sediments can be interpreted in the CS-103-90H-FR seismic line (Fig. 7). Taking into account the average velocity calculated from depth-time curves for this interval, a thickness of about 1200 m may be estimated for the Pliocene sediments. The whole Miocene to Quaternary basin fill thickens towards the basin depocentre, reaching a thickness of ca. 1.6 sec TWT (i.e. ca. 2200 m). A series of extensional faults controlled the accumulation of Pliocene sediments, as demonstrated by the fan geometry observed in the seismic profiles. Although the 3D geometry of the structures cannot be fully constrained, it may be envisaged that these faults are roughly N–S trending, parallel to the main structures bounding the basin at surface. Seismic line CS-103-90H-FR (Fig. 7) shows that, in its central sector, the basin fill is controlled by a W-dipping master fault and associated fault splays located along the axial zone of the Crati River valley. The reflectors interpreted as the possible base of the Pliocene deposits are cumulatively displaced vertically by about 0.5 s TWT, corresponding to a value of about 600 m of vertical offset.

Discussions

Based on the data exposed in this paper, we propose a new tectonic interpretation for the CB within the framework of the regional geological picture of northern Calabria (Fig. 8). In the study area, the oldest marine sediments are Tortonian in age and crop out along both the Tyrrhenian margin of northern Calabria and the Ionian coast, directly overlying crystalline units. At that time, the Sila Massif would have represented part of a wide emerged area supplying clastics to basin areas located both to the west and to the east of the range (Crittelli, 1999). This hypothesis is confirmed by apatite fission track data, indicating exhumation of the Sila block between 35 and 15 Ma (Thomson, 1994). The Messinian sediments, mainly characterized by evaporite facies, extensively cover the Tortonian deposits in the Tyrrhenian offshore. Within the CB Messinian sediments crop out mainly along a narrow belt at the foothills of the Coastal Range and have been found in some wells in the Sibari Plain. This suggests that one or more morpho-structural highs, in part coincident with the present-day Coastal Range, separated the Tyrrhenian basin from a smaller eastern basin during the Late Miocene. These structural highs (proto-Coastal Range in Fig. 8a) represented wide growing anticlines forming along transpressive structures, kinematically linked with NW–SE strike-slip fault zones (like FCFZ and AGFZ in Fig. 1, Tarsi et al., 2007). These anticlines controlled the configuration and the evolution of both the Paola Basin (Pepi et al., 2010) and also the CB. The latter basin, in particular, developed as a large growing syncline, as demonstrated by the overall geometry of the Miocene–Pliocene sediments in the central sector of the basin (seismic line CS-103-90H-FR, Fig. 7).

The Lower Pliocene deposits are of marine type, as suggested by both facies and microfossiliferous data. This could indicate that the proposed morpho-structural high (i.e. the Coastal Range), already partially developed and still growing during the Early Pliocene, divided the Tyrrhenian basin from the proto CB (Fig. 8a, b), which was connected northwards with an open basin (i.e. the Ionian Sea). Evidence of possibly Early Pliocene strike-slip along strike-slip fault zones (i.e. FCFZ and AGFZ in Fig. 8) has been provided by Tarsi et al. (2007). This suggests an ongoing activity of NW–SE trending fault zones and associated structures in this sector of the Calabrian Arc. During the Early Pleistocene the CB was still fed from north. Deposition occurred in a transitional environment (i.e. Gilbert-type fan delta) along the axial part of the basin, hence suggesting a general regressive trend. Early Pleistocene compressional structures in the Sibari Plain are unraveled by seismic interpretation (Fig. 7). These structures probably re-activated older (i.e. Miocene) normal faults. In the field, compressional structures have been observed affecting Lower-Middle Pleistocene deposits within the northernmost part of the CB (Fig. 4b) and along the Pollino Fault (Fig. 4c). Since the Middle Pleistocene (i.e. 700 Ka) a generalized regional uplift affected the entire western sector of the Calabrian Arc (Russo and Schiattarella, 1992; Schiattarella, 1998). This is associated with an extensional tectonic regime recognized throughout the whole southern Apennines (Ortolani et al., 1992; Schiattarella, 1998, 1999).



Fig. 8. Evolution of the Crati Basin and the western sector of northern Calabria. Tectonic sketches (in red structures active at different times) are coupled with the related stratigraphic column: blue areas represent exposed landmass undergoing erosional processes and supplying sediments to both the Tyrrhenian and the Ionian basins. White arrows indicate stress type and approximate orientation for Tyrrhenian off-shore and the Crati Basin. Pollino Fault Zone (PFZ), Pollino San Scil Fault Zone (PSSFZ), Falconara-Cosentino Fault Zone (FCFZ), Amantea-Gimigliano Fault Zone (AGFZ). (a) Sketch showing depocentres and tectonic structures active up to the Late Miocene. The 3D view of the western side of the Coastal Range shows the main attitude of the Late Miocene deposits (filled towards the west), as well as the tectonic contacts between different basement units. W-dipping normal faults offset the original geological contacts. Bleeding attitude, coupled with further geological evidence, confirm that this side of the Coastal Range is coincident with the limb of a regional anticline. (b) Sketch showing structures active up to the Middle-Late Pliocene. (c) Sketch showing structures active up to the Middle Pleistocene. (d) Sketch showing the main sedimentary accumulations and tectonic structures active since Late Pleistocene time. (e) 3D view showing the relationships, at the regional scale, between the Paola Basin, the Coastal Range anticline and the Crati Basin.

From the Middle Pleistocene onwards normal faults started to affect the CB and also the eastern border of the Paola Basin (Pepi et al., 2010, Fig. 8c, d). Nonetheless, a more complex tectonic regime is thought to be active at the Present-day farther to the west in the Tyrrhenian offshore (Pepi et al., 2010, Fig. 8e). Based on the different age of the structures observed within various sectors of the CB, we propose that normal faults bounding the basin propagated mainly towards the north (Fig. 8) as a consequence of the presence of long-lived NW–SE striking strike-slip faults which inhibited their southwards propagation (Fig. 9). In particular, Pizzi and Galadini (2009) demonstrated that pre-existing crustal structures are able to hinder fault re-activation and propagation, therefore controlling the maximum length of Quaternary normal faults in the central and northern Apennines. In the same way, we propose that long-lived fault zones in the northern Calabrian Arc could behave as persistent segment boundaries (sensu Pizzi and Galadini, 2009) and could have partitioned, at a regional scale, the whole regional back-arc extension among a series of extensional basins. Keeping into account the cumulative displacement of the reflectors ascribed to Pleistocene sediments in the central sector of the CB, a vertical strain rate of about 0.9 mm/a may be estimated for the extensional faults controlling the basin architecture since the Middle Pleistocene (i.e. since 700 Ky). The latter value, which is in good agreement with that obtained by Tortorici et al. (1995), has to be considered as a minimum value, because it is not possible to estimate the displacement accumulated along basin bordering normal faults since the Middle Pleistocene.

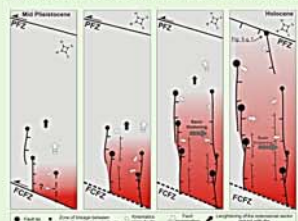


Fig. 9. Time-space propagation of extension within the Crati Basin. Normal faults have formed in the southern part of the basin since the Middle Pleistocene, abutting against the Falconara-Cosentino Fault Zone (FCFZ), and then propagated northwards. During the Late Pleistocene–Holocene, normal faults formed also in the northernmost sector of the basin, where the Pollino Fault Zone (PFZ) was partially re-activated in extension (Spina et al., 2009).

Conclusions

We focused on the architecture of the Crati Basin by integrating geological field data and seismic reflection profiles calibrated by means of deep well logs. The integrated data set allowed us investigating the space-time evolution of the tectonic structures affecting the basin fill from Miocene to Present. The study area is located in the northern portion of the Calabrian Arc, whose evolution was controlled by regional NW–SE trending left-lateral strike-slip faults from Middle Miocene to Middle Pleistocene times. These faults, arranged en-echelon and dissecting the preexisting (Late Oligocene–Early Miocene) orogenic belt, controlled the development of N–S striking, broad antiformal ridges (i.e. the Coastal Range) and associated regional synforms such as those forming the Paola Basin, in the Tyrrhenian offshore, and the Crati Basin onshore. Since the Middle Pleistocene, both E–W and W-dipping normal faults formed in the southernmost sector of the Crati Basin. The inherited regional strike-slip faults became inactive in this sector of the belt and behaved as persistent barriers, inhibiting the southern propagation of the newly formed normal faults. As a consequence, the N–S striking normal faults propagated northward. A blind master fault controls the CB' depocentre in its central and southern sectors. In this zone, the cumulative fault displacement is about 600 m since the Middle Pleistocene, yielding a minimum vertical slip rate of ca. 0.9 mm/a. The integrated, multidisciplinary approach used in this study allowed us obtaining a comprehensive picture of the various stages of development of the Crati Basin, as well as the related structural controls. Our results provide new insights into the tectonic evolution of back-arc zones strongly influenced by wrench faulting, a geodynamic setting that may be envisaged as characterizing areas of extreme arc development and migration, similar to the Calabrian Arc.

References

- Amato, M., 2000. The Calabrian Arc: a review of the geological and tectonic evolution. *Journal of Geological Society of London*, 157, 1–10.
- Amato, M., 2001. The Calabrian Arc: a review of the geological and tectonic evolution. *Journal of Geological Society of London*, 158, 1–10.
- Amato, M., 2002. The Calabrian Arc: a review of the geological and tectonic evolution. *Journal of Geological Society of London*, 159, 1–10.
- Amato, M., 2003. The Calabrian Arc: a review of the geological and tectonic evolution. *Journal of Geological Society of London*, 160, 1–10.
- Amato, M., 2004. The Calabrian Arc: a review of the geological and tectonic evolution. *Journal of Geological Society of London*, 161, 1–10.
- Amato, M., 2005. The Calabrian Arc: a review of the geological and tectonic evolution. *Journal of Geological Society of London*, 162, 1–10.
- Amato, M., 2006. The Calabrian Arc: a review of the geological and tectonic evolution. *Journal of Geological Society of London*, 163, 1–10.
- Amato, M., 2007. The Calabrian Arc: a review of the geological and tectonic evolution. *Journal of Geological Society of London*, 164, 1–10.
- Amato, M., 2008. The Calabrian Arc: a review of the geological and tectonic evolution. *Journal of Geological Society of London*, 165, 1–10.
- Amato, M., 2009. The Calabrian Arc: a review of the geological and tectonic evolution. *Journal of Geological Society of London*, 166, 1–10.
- Amato, M., 2010. The Calabrian Arc: a review of the geological and tectonic evolution. *Journal of Geological Society of London*, 167, 1–10.
- Amato, M., 2011. The Calabrian Arc: a review of the geological and tectonic evolution. *Journal of Geological Society of London*, 168, 1–10.
- Amato, M., 2012. The Calabrian Arc: a review of the geological and tectonic evolution. *Journal of Geological Society of London*, 169, 1–10.
- Amato, M., 2013. The Calabrian Arc: a review of the geological and tectonic evolution. *Journal of Geological Society of London*, 170, 1–10.
- Amato, M., 2014. The Calabrian Arc: a review of the geological and tectonic evolution. *Journal of Geological Society of London*, 171, 1–10.
- Amato, M., 2015. The Calabrian Arc: a review of the geological and tectonic evolution. *Journal of Geological Society of London*, 172, 1–10.
- Amato, M., 2016. The Calabrian Arc: a review of the geological and tectonic evolution. *Journal of Geological Society of London*, 173, 1–10.
- Amato, M., 2017. The Calabrian Arc: a review of the geological and tectonic evolution. *Journal of Geological Society of London*, 174, 1–10.
- Amato, M., 2018. The Calabrian Arc: a review of the geological and tectonic evolution. *Journal of Geological Society of London*, 175, 1–10.
- Amato, M., 2019. The Calabrian Arc: a review of the geological and tectonic evolution. *Journal of Geological Society of London*, 176, 1–10.
- Amato, M., 2020. The Calabrian Arc: a review of the geological and tectonic evolution. *Journal of Geological Society of London*, 177, 1–10.
- Amato, M., 2021. The Calabrian Arc: a review of the geological and tectonic evolution. *Journal of Geological Society of London*, 178, 1–10.
- Amato, M., 2022. The Calabrian Arc: a review of the geological and tectonic evolution. *Journal of Geological Society of London*, 179, 1–10.
- Amato, M., 2023. The Calabrian Arc: a review of the geological and tectonic evolution. *Journal of Geological Society of London*, 180, 1–10.
- Amato, M., 2024. The Calabrian Arc: a review of the geological and tectonic evolution. *Journal of Geological Society of London*, 181, 1–10.
- Amato, M., 2025. The Calabrian Arc: a review of the geological and tectonic evolution. *Journal of Geological Society of London*, 182, 1–10.